Field Behavior and Modeling of Cracked-and-Seated Semirigid Pavement After Rehabilitation

MORRIS DE BEER, EDUARD G. KLEYN, AND HERMAN WOLFF

Discussed are the structural behavior and subsequent modeling of a typical rehabilitation pavement design of a pavement with stabilized layers (semirigid) in South Africa. The rehabilitation consists of a 150-mm, high-quality crushed stone on a pre-cracked-and-seated semirigid pavement. Its structural behavior was determined through full-scale accelerated testing with a heavy vehicle simulator and associated technology. The modeling was done with a nonlinear, multilayer finite element method. Typical results are given, together with detailed modeling of the pavement response. A manual method for backcalculation of nonlinear granular material properties based on multidepth deflection measurements was used successfully to fit the full deflection basins at different depths within the pavement structure.

Recent trends in South Africa regarding road infrastructure funding necessitate improved pavement rehabilitation design and evaluation methods. As most of southern Africa is relatively dry, the use of thick (> 150 mm) flexible asphalt bases in road pavements is limited. Semirigid pavements are more popular, especially in the former province of the Transvaal, where more than 80 percent of the pavements incorporate stabilized (cementitious) base or subbase layers with relatively thin (< 50 mm) asphalt surfacing or normal surface treatments, or both. Pavement research during the past 7 years has been aimed primarily at reducing the gap between theory and practice. Detailed studies of failure mechanisms and structural behavior have been conducted and suitable transfer functions for the designer developed with the aid of full-scale accelerated tests using a South African heavy vehicle simulator (HVS) belonging to the Roads Branch of the Transvaal Provincial Administration (TPA). Studies of existing pavements as well as of several rehabilitation strategies were made (*1–3*).

In this paper some behavioral and modeling aspects of a typical heavy rehabilitation of an original pavement with portland blast furnace cement–stabilized layers are discussed. The rehabilitation option involves a 150-mm high-quality crushed stone base on the pre-cracked-and-seated semirigid pavement structure. [Another rehabilitation option of 35-mm asphalt surfacing on the cracked-and-seated stabilized layers was also investigated during this project and was analyzed with the mechano-lattice method (*4*). This work, however, is reported elsewhere (*5*).] Aspects such as permanent deformation and resilient response are addressed, both during a so-called crack-and-seat operation and subsequent HVS testing.

The pavement response to traffic loading was modeled with nonlinear stress-dependent layer moduli using the finite element method for the crushed stone base layer section. The study determined that multidepth deflection measurements with the multidepth deflectometer (MDD) (*6,7*) are ideally suited for the backcalculation of granular and sublayer material properties to represent measured deflection basins on these pavements. Further, the study also indicates that plastic deformation measured by the MDD system can be used to aid in the prediction of potential cracking in thin asphalt surfacings. The latter, however, is discussed elsewhere (*5*).

Both the field quantification of structural behavior with the HVS and the subsequent modeling provided the designers as well as the road authority with adequate data, and models with a relatively high degree of confidence, to address effectively infrastructure needs of the next decade in southern Africa.

M. de Beer, Division of Roads and Transport Technology, CSIR, P.O. Box 395, Pretoria 0001, South Africa. E. Kleyn, Roads Branch, Transvaal Provincial Administration, Pretoria, South Africa. H. Wolff, Theron Prinsloo Grimshell & Pullen (Durban) Consulting Engineers, Durban, South Africa.

PREPARING REHABILITATION SECTIONS

Background

During studies using HVS technology on existing pavement and similar structures indicated in Figure 1, several important aspects regarding structural behavior mechanisms of these pavements were identified. The purpose of this paper, however, is not to describe these aspects in detail, although reference will be made occasionally to some of the more important mechanisms. The mechanisms are also summarized by De Beer elsewhere (*2,8*). They include effective fatigue life, (*Nef*), and crushing failure, (*Nc*) of lightly stabilized base or subbase layers with relatively thin asphalt surfacings. The specific structure in Figure 1 was classified as a relatively shallow pavement structure using the dynamic cone penetrometer (DCP) technology (*9,10*). Hence, fatigue failure of the base is most likely to be the dominant failure mechanism of this pavement. Another interesting fact about this pavement is that a relatively softer interlayer, by DCP definition, was found between the base and subbase.

The existence of this interlayer can be attributed to two factors: poor construction (mixing) of the stabilizer, and possible carbonation of the stabilized subbase layers (*11*). HVS tests indicated fatigue failure after 1 million standard (80-kN) axles (MISA), after which the rate of permanent deformation increased from approximately 2.27 mm/MISA to 10 mm/MISA. Cracking in the conventional double seal also started at this failure point. HVS tests at higher loads displayed relatively short fatigue lives for these pavements, indicating a relatively high load sensitivity for fatigue failure. From these basic structural performance data, and taking into account the risk of overloading in South Africa, it was decided to

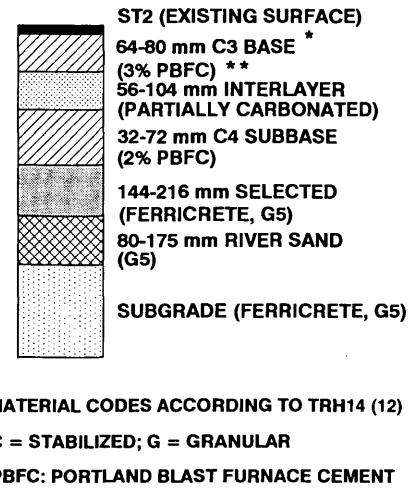

FIGURE 1 Existing pavement structure before crack-and-seat operation.

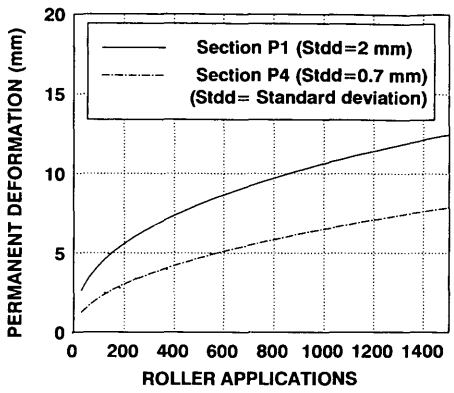

FIGURE 2 Permanent deformation during crack-and-seat operation.

study various rehabilitation options for this kind of pavement. The relatively small HVS test section (1 m by 8 m) was considered too small for a proper rehabilitation investigation. The authors decided to use a so-called crack-and-seat method to convert relatively large pavement areas (40 m by 3.5 m, Section P1; 80 m by 3.5 m, Section P4) of originally stabilized layers from the pre- to the post-cracked state (similar to that established with the HVS), using an 8-ton vibratory roller.

Crack-and-Seat Operation

Permanent deformation measured with the rod-and-level method and resilient surface deflections measured with a modified Benkelman beam were used for control measurements during the crack-and-seat operation (*1*). Figure 2 shows the permanent deformation during the crack-and-seat operation on these two sections, and Figure 3 shows the resilient standard 40-kN maximum deflections before and after the rolling. Not only did deflections increase, but so did variability because of the cracked state of the stabilized material. The stabilized material was broken down into blocks of varying sizes from 150-mm blocks to relatively large blocks of over 500 mm (as determined visually). Cracks were found to be often plane-like (oblique to horizontal) cracks rather than classical vertical fatigue cracks, similar to those that were found after HVS testing. After the crack-and-seat operation, the upper 20 to 30 mm was completely pulverized and manually removed with brooms before the 150-mm crushed stone dolomite base was constructed of G1-base material [Technical Recommendations for Highways 14 (*12*)], with a coarse (13-mm) single seal and sand slurry. Standard 80-kN axle road surface maximum deflections after the G1-base construction varied between 200 and 400 μm (see Figure 3).

HVS TESTING ON REHABILITATED SECTIONS

Permanent Deformation

Figure 4 shows measured permanent deformations at various stages of HVS testing on a crushed stone (G1-base) section (Section 339A4). During the dry state, relatively little plastic or permanent deformation (rut) was measured (approximately 2 mm). The initial rut of 2 to 3 mm existed primarily within the single seal, including the sand slurry (the slurry was used to provide a relatively smooth surface for rut measurements on the HVS test section). No difference occurred between the upper two curves, indicating no local failure around the MDD positions during testing in the dry state. After the artificial introduction of water onto the pavement at approximately 3.7 MISA, local failure around the MDD positions occurred. During the dry state (N < 3.7 MISA), the rate of deformation was approximately 0.54 mm/MISA and increased to 6.76 mm/MISA during the wet state on the basis of the average rut. At a wheel load of 70 kN the rate of deformation also increased in both the dry and wet conditions. The relative damage based on the well-known power law (*13*) was calculated and the average relative damage exponent, d, for this section is 2.31 for dry and 2.44 for wet conditions (see Equation 1). No cracks other than those around the MDDs and the DCP test positions appeared in this section; the majority of the deformation resulted from stone loss from the surfacing.

$$D_l = (P/40)^d \quad (1)$$

where

D_l = relative damage factor,
d = relative damage exponent, and
P = test wheel load in kilonewtons.

Nuclear density measured before and after the HVS test indicated that a slight increase (2.2 percent) in dry densities had occurred (or 87.7 to 89.9 percent of apparent density) as a result of HVS trafficking. During this period, the average moisture content also increased from approximately 1.8 percent to between 3 and 4 percent as a result of surface water ingress. Figure 5 shows permanent deformation measured at different depths with an MDD system within the pavement and indicates that approximately 50 percent of the deformation occurred within the base. However, upon inspection most of the rutting appeared to occur within the sand slurry seal. After water was introduced, permanent deformation increased dramatically, mainly as a result of failure around the MDD holes.

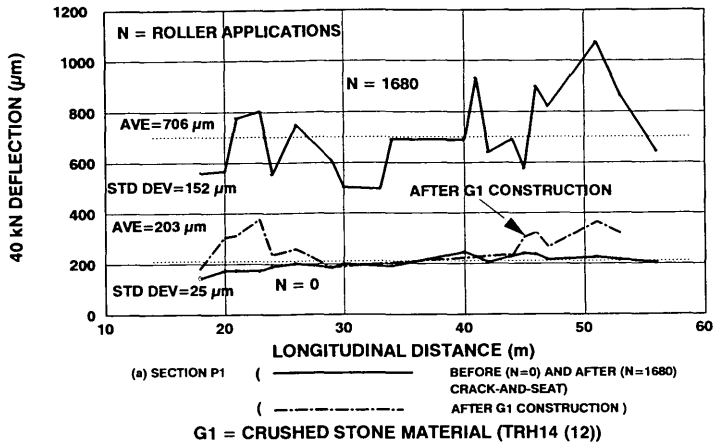

FIGURE 3 Increase in maximum road surface deflection as result of roller applications.

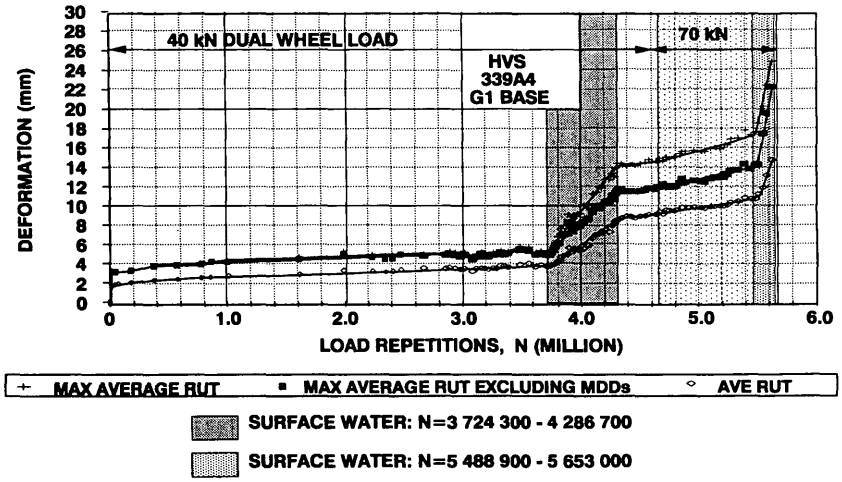

FIGURE 4 Permanent deformation on crushed stone base pavement section.

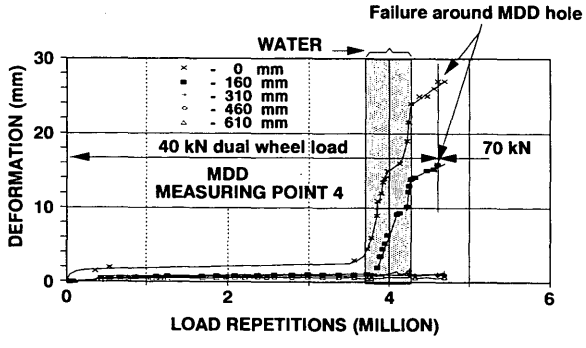

FIGURE 5 Permanent deformation at different depths in crushed stone pavement section.

Resilient Response

Figure 6 illustrates resilient deflection at various stages of trafficking on the G1-base section. The initial 40-kN maximum deflection was approximately 330 μm, and it increased to a steady level (upper limit) at around 500 μm. According to TPA practice, threshold and warning levels of maximum standard deflection are between 300 and 400 μm, respectively. An increase in deflection to approximately 640 μm occurred during the wet test. Figure 7 illustrates the standard 40-kN maximum depth deflections from the MDDs at the start of the test and after 3.67 MISA. Very few changes in depth deflections occurred during the test. The actual measured deflection basins at different depths are given in Tables 1 and 2. An increase in relative deflection within the crushed stone

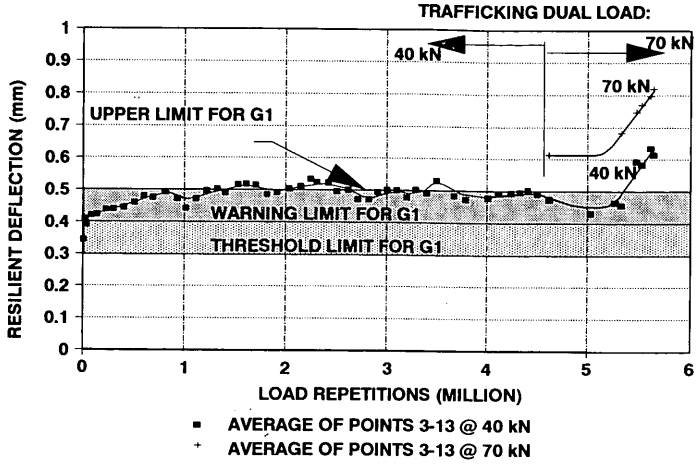

FIGURE 6 Average road surface deflection on crushed stone base pavement at various stages of HVS testing.

base was measured as well as an increase in subgrade deflection. Measurements on the MDD anchor showed that there was no movement under loading, and extrapolation of MDD deflections at depths of 460 and 610 mm was used to calculate the zero deflection level (ZDL), also referred to as depth to "apparent rigid layer" (*14*). Pavement modeling using the MDD depth deflection basin measurement as well as the maximum road surface deflection was applied to backcalculate layer and material properties, which are discussed later.

Modeling of Crushed Stone Pavement

Modeling of the crushed stone base pavement section was done primarily with the MICH-PAVE finite element code developed by Harichandran and Yeh (*15*). The crushed stone layer was modeled using the well-known stress dependent model:

$$Mr = K1\Theta^{K2} \tag{2}$$

where $\Theta = \sigma_1 + \sigma_2 + \sigma_3$ and $K1$, $K2$ are material constants.

The rest of the pavement was divided into three layers, with a rigid layer, represented by a relatively stiff layer ($E6$ = 35 000 MPa) at a depth (ZDL), calculated from MDD measurements (Figure 7). The backcalculated material and layer properties for the two stages of HVS trafficking are summarized in Figure 8. Figures 9 and 10 show the measured and calculated deflection basins. At the time of this study, the backcalculation was done manually, which was very time consuming. However, the method of a flexible boundary used within the MICH-PAVE code (*15*) was approximately 14 times faster than the manual ILLI-PAVE code

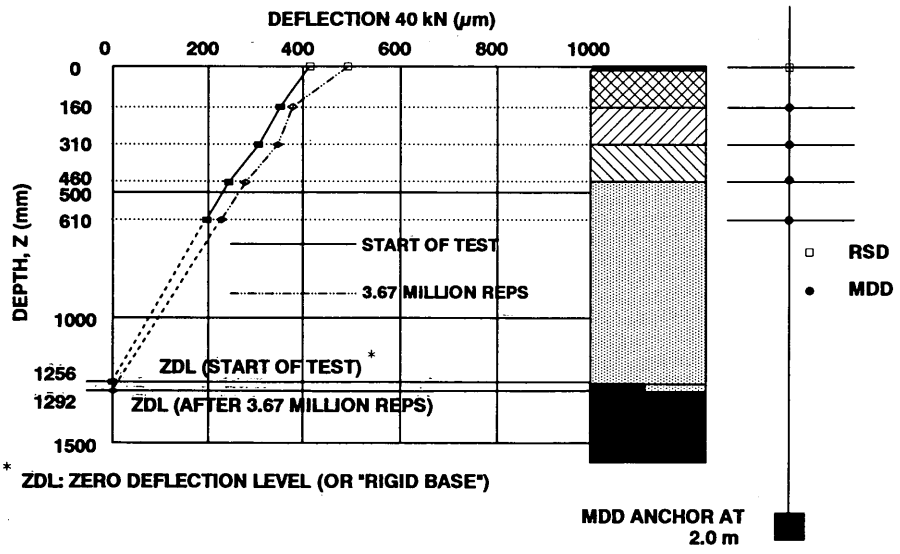

FIGURE 7 Multidepth deflectometer deflection at two stages of HVS trafficking on crushed stone pavement structure.

TABLE 1 Measured and Predicted Deflections (μm) at Start of HVS Testing on Crushed Stone Section

DEPTH (mm)													
0 Measured Deflection	413.03												
Predicted Deflection	413.00												
Horizontal Dist (mm)	0	29.25	58.5	87.75	117	175.5	234	292.5	380.25	468	585	731.25	906.75
160 Measured Deflection		349.45	341.81	333.71	323.26	299.89	276.14	251.14	203.11	163.76	118.19	80.49	45.03
Predicted Deflection		348.51	342.52	332.78	319.96	290.15	259.40	226.68	187.00	151.34	108.47	70.43	24.11
Error (%)		-0.27	0.21	-0.28	-1.02	-3.25	-6.06	-9.47	-7.93	-7.59	-8.22	-12.50	-16.47
ABS error (μm)		-0.94	0.71	-0.92	-3.30	-9.74	-16.74	-24.46	-16.11	-12.42	-9.72	-10.16	-20.92
RMSE (%)		0.16											
RMSE 1 (%)*		0.07											
310 Measured Deflection		303.89	299.31	293.21	287.74	269.09	252.49	233.79	198.04	160.29	117.31	82.24	48.39
Predicted Deflection		303.25	299.85	294.29	286.61	266.99	244.81	220.00	183.33	149.30	107.47	69.79	23.87
Error (%)		-0.21	0.18	0.37	-0.39	-0.78	-3.04	-5.90	-7.43	-6.86	-8.39	-15.14	-50.68
ABS error (μm)		-0.64	0.54	1.08	-1.13	-2.10	-17.68	-13.79	-14.71	-10.99	-9.84	-12.45	-24.52
RMSE (%)		0.17											
RMSE 1 (%)		0.06											
460 Measured Deflection		240.23	237.21	234.06	232.53	221.34	210.69	196.46	171.23	145.71	112.23	83.01	50.63
Predicted Deflection		242.65	240.80	237.76	233.32	221.52	207.31	192.08	163.67	136.23	99.22	64.44	21.73
Error (%)		1.01	1.51	1.58	0.34	0.08	-1.60	-2.23	-4.42	-6.51	-11.60	-23.11	-57.08
ABS error (μm)		2.42	3.59	3.70	0.79	0.18	-3.37	-4.38	-7.56	-9.48	-13.01	-19.37	-28.90
RMSE (%)		0.19											
RMSE 1 (%)		0.08											
610 Measured Deflection		195.90	195.35	193.82	191.01	186.32	177.88	169.33	151.20	134.00	103.4	79.73	50.11
Predicted Deflection		197.27	196.10	194.15	191.29	183.36	173.55	163.64	142.71	121.44	91.84	62.49	24.37
Error (%)		0.70	0.39	0.17	0.14	-1.59	-2.43	-3.36	-5.61	-9.37	-11.18	-21.63	-51.37
ABS error (μm)		1.37	0.75	0.33	0.28	-2.96	-4.33	-5.69	-8.49	-12.56	-11.56	-17.24	-25.74
RMSE (%)		0.18											
RMSE 1 (%)		0.08											

NOTE: Load 40 kN; tire pressure 520 kPa.

*RMSE 1 *excludes* data at horizontal distance 906.75 mm, RMSE includes data at horizontal distance 906.75 mm.

TABLE 2 Measured and Predicted Deflections (μm) After 3.67 Million Load Repetitions on Crushed Stone Section

DEPTH (mm)													
0 Measured Deflection	489.73												
Predicted Deflection	489.00												
Horizontal Dist(mm)	0	29.25	58.5	87.75	117	175.5	234	292.5	380.25	468	585	731.25	906.75
160 Measured Deflection		375.23	369.60	359.60	347.85	320.30	285.23	249.25	198.23	156.08	110.55	68.43	38.18
Predicted Deflection		376.60	370.39	360.59	347.84	317.40	285.26	253.01	209.40	168.94	121.94	76.11	42.43
Error (%)		0.37	0.28	0.37	-0.00	-0.91	-0.01	1.51	5.64	8.24	10.30	11.23	11.15
ABS error (μm)		1.37	1.04	1.32	-0.01	-2.90	-0.03	3.76	11.18	12.87	11.39	7.69	4.26
RMSE (%)		0.62											
310 Measured Deflection		345.68	336.28	332.19	324.18	312.08	238.90	261.20	217.98	174.30	128.38	82.85	48.43
Predicted Deflection		345.56	341.77	335.68	326.75	304.21	277.60	249.22	207.89	168.46	122.13	76.49	42.92
Error (%)		-0.03	1.63	1.05	0.79	-2.58	-4.24	-4.59	-4.63	-3.35	-4.87	-7.68	-11.36
ABS error (μm)		-0.11	5.50	3.49	2.57	-8.05	-12.30	-11.98	-10.08	-5.84	-6.25	-6.36	-5.50
RMSE (%)		0.50											
460 Measured Deflection		276.19	274.11	271.09	265.94	254.46	237.39	217.01	183.76	151.09	112.11	72.34	43.14
Predicted Deflection		277.78	275.50	271.97	266.78	252.70	235.70	216.14	184.83	152.92	113.75	72.92	43.02
Error (%)		0.57	0.51	0.33	0.32	-0.69	-0.71	-0.40	0.58	1.21	1.46	0.81	-0.27
ABS error (μm)		1.59	1.39	0.88	0.85	-1.77	-1.68	-0.87	1.07	1.83	1.64	0.58	-0.12
RMSE (%)		0.07											
610 Measured Deflection		227.25	226.80	225.30	222.65	215.80	205.85	190.90	162.10	132.10	99.60	65.15	37.30
Predicted Deflection		228.66	227.18	224.82	221.30	211.42	199.14	184.79	161.28	136.12	104.20	70.37	41.38
Error (%)		0.62	0.17	-0.21	-0.61	-2.03	-3.26	-3.20	-0.50	3.05	4.62	8.03	10.95
ABS error (μm)		1.41	0.38	-0.48	-1.35	-4.38	-6.71	-6.10	-0.81	4.02	4.61	5.23	4.08
RMSE (%)		0.45											

NOTE: Load 40 kN; tire pressure 520 kPa.

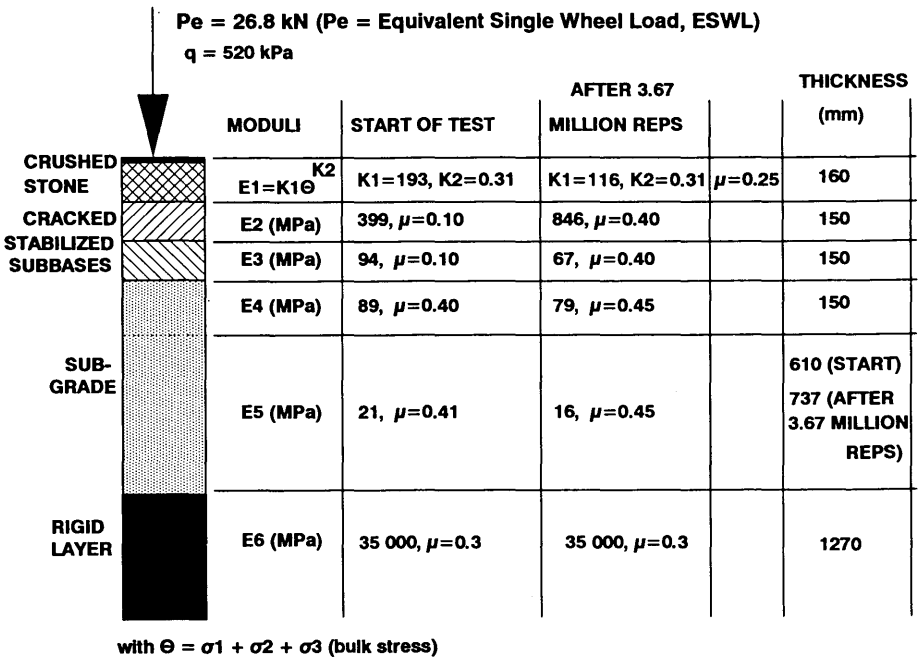

MODULI	START OF TEST	AFTER 3.67 MILLION REPS		THICKNESS (mm)
$E1=K1\Theta^{K2}$	K1=193, K2=0.31	K1=116, K2=0.31	μ=0.25	160
E2 (MPa)	399, μ=0.10	846, μ=0.40		150
E3 (MPa)	94, μ=0.10	67, μ=0.40		150
E4 (MPa)	89, μ=0.40	79, μ=0.45		150
E5 (MPa)	21, μ=0.41	16, μ=0.45		610 (START) 737 (AFTER 3.67 MILLION REPS)
E6 (MPa)	35 000, μ=0.3	35 000, μ=0.3		1270

FIGURE 8 Model parameters for crushed stone pavement structure (moduli in megapascals).

method (*16*). In the case discussed here, the flexible boundary with MICH-PAVE was placed at a depth of approximately 2.54 m. In this analysis, parameters $K1$ of the granular base and $E2$ to $E5$, including the Poisson's ratios for the various layers, were changed manually until measured and calculated deflections converged. In both sets of MDD basin measurements, the root-mean-square error (RMSE) percentage (*14*) varied between 0.01 and 0.70. Absolute errors were less than 33 μm, with maximum percentage errors less than 13. During the analysis of the measured deflection basins it was found that the surface deflection basin measured with the road surface deflectometer (RSD) (modified Benkelman beam) did not exactly coincide with those measured with the MDD module at the surface of the pavement. Although the maximum deflections were similar, the shape of the basin was different, the RSD basin measured relatively higher deflections, especially from a distance of 250 mm from the load toward the tail end of the basin. Because of these differences, which were believed to be related to the different reference systems (geometry) of the two deflection measurement systems—RSD referenced on surface, MDD referenced in depth—only the maximum RSD deflection together with the MDD depth deflection basin results were used in this study for backanalysis. See Figures 9 and 10.

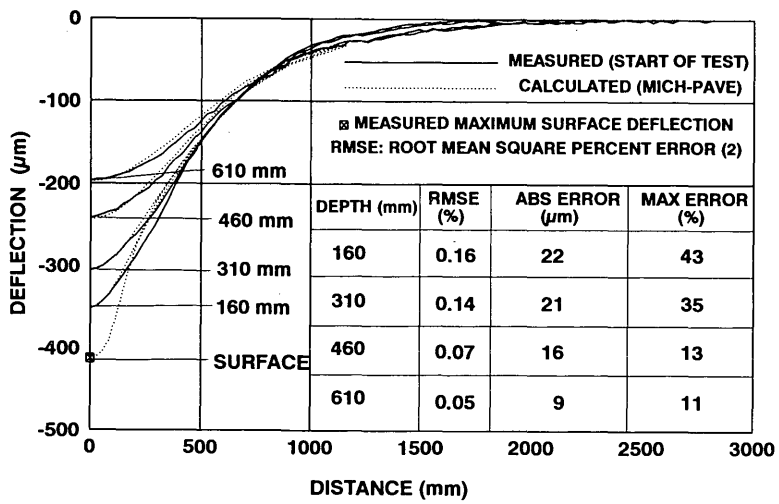

DEPTH (mm)	RMSE (%)	ABS ERROR (μm)	MAX ERROR (%)
160	0.16	22	43
310	0.14	21	35
460	0.07	16	13
610	0.05	9	11

FIGURE 9 Measured and calculated deflection basins at start of HVS testing on crushed stone section. (For actual deflections, see Tables 1 and 2.)

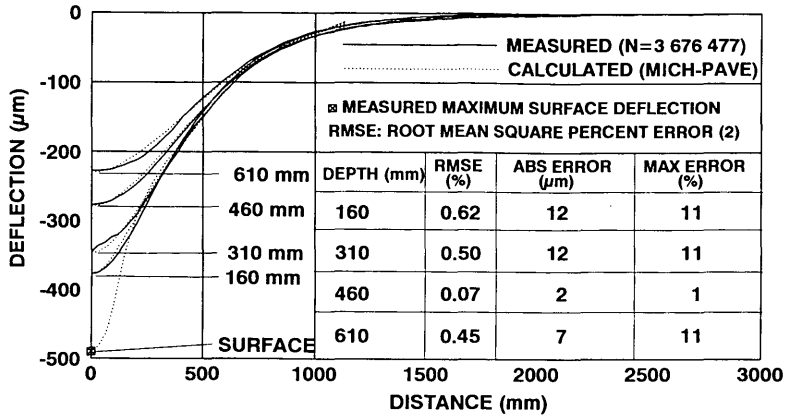

DEPTH (mm)	RMSE (%)	ABS ERROR (μm)	MAX ERROR (%)
160	0.62	12	11
310	0.50	12	11
460	0.07	2	1
610	0.45	7	11

FIGURE 10 Measured and calculated deflection basins after 3.67-million load repetitions on crushed stone section. (For actual deflections, see Tables 1 and 2.)

Discussion of Model Properties

It was found the $K1$ decreased from 193 to 116 MPa (−40 percent) as a result of HVS trafficking and a possible increase in moisture content of the granular material. The $K2$ appeared to be constant at a value of 0.31, as well as Poisson's ratio μ = 0.25 (see Figure 8). The $K2$ and μ compare favorably with tentative laboratory values determined with the K-mold rapid triaxial test proposed by Semmelink (*17,18*). It is believed that these constants may change slightly with improved surface basin measurements. At this stage, however, it is clear that the increase in surface deflection was primarily the result of a reduction in the $K1$ value of the crushed stone material. This reduction in $K1$ also effectively reduced the load-bearing capacity of the base layer, hence the higher deflections in the lower (subgrade) layers. Regarding the cracked-and-seated stabilized subbase layers (in the equivalent granular state), it was found that a two-layer linear elastic system with a modular ratio varying between 4.2 and 12.6 was needed to reproduce the best-fit basins in this case. That might be an indication of relatively strong stress dependency within these layers. Modeling these layers (or a single equivalent granular layer) using the crushed stone stress-dependent model could also produce acceptable basins. However, that approach was not pursued for this study because of uncertainty of acceptable $K2$ values for cracked stabilized material and also in order to limit the number of unknowns during the iteration process.

As a result of trafficking (traffic molding) it appeared that the modular ratio increased threefold, resulting in higher moduli for the upper stabilized layer and lower moduli for the lower layer (suggesting a possible reduction in $K1$ and an increase in $K2$ if the crushed stone stress-dependent model is assumed). In this case, a change in Poisson's ratio of both stabilized layers from 0.10 to 0.40 was also needed to reduce the RMSE of each basin. The reason for the increase in Poisson's ratio is not clear, but is believed to be related to a possible advanced state of cracking (more granular) of the already cracked stabilized layers, as well as possible "model dependency' of these values. Future research perhaps should aim to improve in situ methods for obtaining effective Poisson's ratios for backcalculation.

Finally, the authors found it was best to divide the subgrade into two layers (Layer 4 and Layer 5) on top of the relatively shallow rigid layer. If the subgrade is modeled as one layer with the rigid layer in place, the deflection at a depth of 610 mm is grossly underestimated. This finding is confirmed by Rohde (*14*). The modulus of Layer 4 was 89 MPa, and it was reduced to 79 MPa (−11 percent), probably as a result of increased deflection in the pavement structure. Poisson's ratio changed from 0.4 to 0.45. The second subgrade layer (Layer 5) modulus was 21 MPa at the start of test and changed to 16 MPa, with the Poisson's ratio changing from 0.41 to 0.45.

Although it is understood that these layer properties are model dependent, it is shown here that the layer properties can be used to reproduce deflections measured within the pavement system relatively accurately. Future research, however, should be directed at model-independent parameters and properties obtained through backcalculation.

SUMMARY AND CONCLUSIONS

In this paper, the structural behavior of a typical rehabilitated pavement structure with semirigid subbase layers is discussed. The structural behavior was quantified using HVS technology. The pavement structure involved a 150-mm crushed stone base on a cracked-and-seated lightly stabilized subbase layer. Detailed resilient modeling of the crushed stone base section was done with nonlinear finite element analysis. Measured resilient deflections at various depths in the pavement were used as input to model the behavior of the pavement.

The study indicated that results from full-scale accelerated testing (e.g., HVS) and MDD technology applied to pavement systems with varying materials (including semirigid layers) can assist with the input parameters for modeling pavement structure responses. Although some refinements in the model and measuring techniques are still needed, the methods adopted here strive to narrow the gap between theory and practice.

More emphasis should be given to the accurate measuring of surface deflection basins in association with multidepth deflection basin measurements. Further, nonlinear multilayer backcalculation techniques should be computerized to determine (backcalculate) in situ material and layer properties on a wider and more practical basis. However, full-scale research should be accompanied by de-

velopment of rapid laboratory testing methods for determining relevant material constitutive laws. The new rapid triaxial test is such a development (i.e., the so-called *K*-mold) (*17,18*), wherein the horizontal stress, σ_3, is mobilized automatically from application of the vertical stress, σ_1. From this test, stress-dependent moduli and Poisson's ratio can be determined, as well as Mohr-Coulomb parameters, in less than 1 min.

Implementation of the methods and findings summarized in this study will ensure more economical rehabilitation designs for semi-rigid pavement structures in southern Africa.

ACKNOWLEDGMENT

The authors thank both the Roads Branch of the Transvaal Provincial Administration (TPA) and the Director of the Division of Roads and Transport Technology for their support during this research and for permission to publish this paper.

REFERENCES

1. De Beer, M., E. G. Kleyn, H. Wolff, and J. R. Otte. Behaviour of Various Rehabilitation Options of a Cracked-and-Seated Semi-Rigid Pavement During Accelerated Testing in Transvaal. *Proc., 1991 Annual Transportation Convention*, Vol. 4B, Aug. 1991, 23 pp.
2. De Beer, M. *Aspects of the Design and Behavior of Road Structures Incorporating Lightly Cementitious Layers.* Ph.d dissertation. Department of Civil Engineering, University of Pretoria, Pretoria, South Africa, 1990.
3. Kleyn, E. G., C. R. Freeme, and L. J. Terblanche. The Impact of Heavy Vehicle Simulator Testing in Transvaal. *Proc., 1985 Annual Transportation Convention*, Pretoria, South Africa, 1985.
4. Yandell, W. O. *Mechano-Lattice Analysis.* Lecture Notes, LGI Short course, University of Pretoria, South Africa, 1990.
5. De Beer, M., E. G. Kleyn, and H. Wolff. *Field Behaviour and Modelling of a Cracked-and-Seated Semi-Rigid Pavement after Rehabilitation.* Research Report DPVT 221. Division of Roads and Transport Technology, CSIR, Pretoria, South Africa, March 1994.
6. De Beer, M., E. Horak, and A. T. Visser. The Multi-Depth Deflectometer (MDD) System for determining the Effective Elastic Moduli of Pavement Layers. In *1st Proc., International Symposium on Nondestructive Testing of Pavements and Backcalculation of Moduli*, Special Technical Publication 1026, ASTM, Philadelphia, Pa., 1988.
7. De Beer, M. Pavement Response Measuring System. *Proc., 2nd International Symposium*, West Lebanon, N.H. Sept. 1991.
8. De Beer, M. Developments in the South African Mechanistic Design Procedure for Asphalt Pavements. *Proc., 7th International Conference on Asphalt Pavements: Design Construction and Performance, Vol. 3*, University of Nottingham, England, Aug. 1992, pp. 54–76.
9. De Beer, M., E. G. Kleyn, and P. F. Savage. Towards a Classification System for the Strength-Balance of Thin Surfaced Flexible Pavements. *Proc., 1988 Annual Transportation Convention, Vol. 3D*, Pretoria, South Africa, July 1988.
10. De Beer, M. Use of the Dynamic Cone Penetrometer (DCP) in the Design of Road Structures. Presented at *10th African Regional Conference on Soil Mechanics and Foundation Engineering*, Maseru, Lesotho, South Africa, Sept. 1991.
11. Netterberg, F., and P. Paige-Green. *Carbonation of Lime and Cement Stabilised Layers in Road Construction.* Technical Report RS/3/84. NITRR, Council for Scientific and Industrial Research, Pretoria, South Africa, 1984.
12. *Guidelines for Road Construction Materials.* Technical Recommendations for Highways, TRH14, Committee of State Road Authorities, Department of Transport, Pretoria, South Africa, 1985.
13. Irick, P. E., and W. R. Hudson. *NCHRP Report 2A: Guidelines for Satellite Studies of Pavement Performance.* HRB, National Research Council, Washington, D.C., 1964.
14. Rohde, G. T. *The Mechanistic Analysis of Pavement Defections on Subgrades Varying in Stiffness with Depth.* Ph.d. dissertation. Texas A&M University, College Station, Dec. 1990.
15. Harichandran, R. S., and M. S. Yeh. Flexible Boundary in Finite-Element Analysis of Pavements. In *Transportation Research Record 1207*, TRB, National Research Council, Washington, D.C., 1988, pp. 50–60.
16. *ILLI-PAVE Users Manual.* Department of Civil Engineering, University of Illinois at Urbana-Champaign, 1986.
17. Semmelink, C. J. The Use of the DRTT K-Mould in Determining the Elastic Moduli of Untreated Roadbuilding Material. *Proc., 1991 Annual Transport Convention, Paper 6*, Pretoria, South Africa, 1991, 14 pp.
18. Semmelink, C. J., and M. De Beer. Development of a Dynamic DRTT K-Mould System. *Proc., 13th Annual Transportation Convention*, University of Pretoria, South Africa, June 28 to July 1, 1993.

Publication of this paper sponsored by Committee on Modelling Techniques in Geomechanics.